Received: 27 March 2017 | Revised: 29 June 2017 | Accepted: 25 September 2017

DOI: 10.1111/ter.12301

PAPER

WILEY Terra Nova

Towards global space geodetic mapping of the dynamic deformation field after great earthquakes

Gyula Grenerczy[1] | Tamás Jámbor[1] | Seth Stein[2] | Péter Farkas[1] | Marcell Ferenc[3]

[1]Institute of Geodesy Cartography and Remote Sensing, Satellite Geodetic Observatory, Budapest, Hungary

[2]Department of Earth and Planetary Sciences, Northwestern University, Evanston, IL, USA

[3]Conservatoire National des Arts et Métiers, École Supérieure des Géomètres et Topographes, Paris, France

Correspondence
Dr. Gyula Grenerczy, Satellite Geodetic Observatory, Institute of Geodesy Cartography and Remote Sensing, Budapest, Hungary.
Email: grener@caesar.elte.hu

Abstract

GPS systems can be used as seismometers by sampling ground positions to detect travelling seismic waves. Data from dense geodetic networks near large earthquakes have been used to improve magnitude estimates, for tsunami warning, and to better understand the rupture processes. Here, we present 1 Hz GPS records of the March 11th, 2011, Mw = 9.0 Tohoku earthquake at unprecedented teleseismic distances. The spatial and temporal variations of the three-dimensional GPS displacement vector field show various body waves, Love and Rayleigh surface waves along the direct path, and Love waves from the more than 31 000 km long major arc path. These results suggest that seismic wavefields can be mapped at teleseismic distances globally using space geodesy and could thus be used for source and structural studies. Data from numerous real-time kinematic GPS networks could be combined to show the displacement field, giving unparalleled views of Earth's response to large earthquakes.

1 | INTRODUCTION

The feasibility of using high rate GPS observations for monitoring seismic waves was proposed in the 1990s (Hirahara, Nakano, Hoso, Matsuo, & Obana, 1994) and demonstrated (Larson, Bodin, & Gomberg, 2003) using GPS seismograms from the magnitude 7.9 Denali event of November 3, 2002. Subsequently, GPS seismograms from large earthquakes have been analysed (Hardebeck et al., 2004; Miyazaki et al., 2004), yielding some distant detections of surface waves (Kouba, 2005; Vigny et al., 2005). Laboratory simulation (Elósegui, Davis, Oberlander, Baena, & Ekström, 2006), involving moving a GPS antenna on a shake table, showed that the resulting GPS seismograms were accurate to a few mm. GPS seismology complements broadband seismometers, because it directly measures displacement without saturation, clipping and drift. The technique is drawing increasing interest due to the growing number of GPS networks reporting positions in real time. In particular, efforts are being made to combine real-time GPS and seismic data because GPS more accurately measures displacement for very large events (Emore, Haase, Choi, Larson, & Yamagiwa, 2007). After the 2011 March 11 Mw 9.0 Tohoku earthquake, 30 sec. kinematic position estimates of the Japanese GEONET GPS network data were analysed (Grapenthin & Freymueller, 2011) to map near-field seismic displacements, providing not only time series of several stations but also a vector record of the seismic deformation and wavefield. For this earthquake, we studied the 100 times smaller displacements recorded at extreme distances – 9,000 km and 31,000 km – using 1 sec. data from a GPS network in the Pannonian Basin, Hungary (Figure 1). The data show the full displacement vector fields of travelling body waves, Love and Rayleigh surface waves along the direct source–receiver path, and Love waves from the major arc path. This complete three-dimensional vector field record of dynamic deformation of seismic waves at these large distances shows that space geodetic mapping of global deformation fields after great earthquakes is feasible.

2 | DATA

The Pannonian Basin GPS network contains 35 geographically more-or-less-evenly distributed stations providing 1 Hz GPS data. Most sites are located on Quaternary loose sediments on rods and pillars

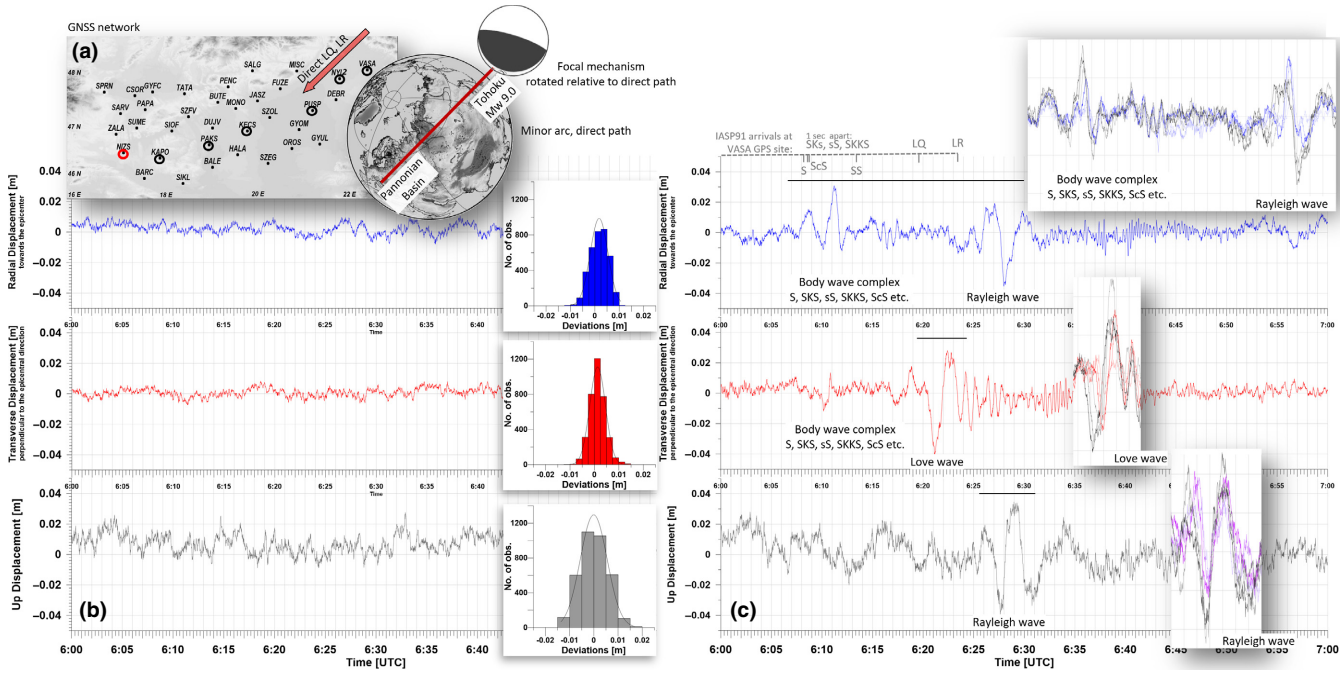

FIGURE 1 (a) GPS site distribution and geometry relative to the Tohoku earthquake, focal mechanism (Nettles, Ekström, & Koss, 2011) rotated to radial direction, 42° azimuth, shown with an arrow on the globe. (b) 1-hour unfiltered 1Hz time series of VASA GPS station for three components on the day before the earthquake together with scatter of kinematic coordinate estimates on histograms. (c) GPS seismograms of the Tohoku earthquake. Inserts are enlarged parts of GPS seismograms for six sites located along the surface-wave travel path (top right)

atop buildings in urban areas. Results were obtained using the BERNESE GPS Software Version 5.0 (Dach, Hugentobler, Fridez, & Meindl, 2007). We applied precise satellite orbits and Earth rotation parameters from the International GNSS Service, an ionosphere model from the Center for Orbit Determination, and ocean loading from the FES2004 model (Lyard, Lefevre, Letellier, & Francis, 2006). Reference data are the daily coordinates of the GNSS sites based on previous 24-hour data. The reference frame was the 2005 realization of the International Terrestrial Reference Frame (Altamimi, Collilieux, Legrand, Garayt, & Boucher, 2007). Our data processing uses double differencing (DD) of single differenced observations between two stations where the measured phase is differenced at a station between two simultaneously observed satellites. The GPS data were processed as vectors to a reference site (NIZS, farthest from the epicentre) rather than individually (Precise Point Positioning). DD processing greatly reduces several errors (clock, orbit, atmosphere, noise etc). We used elevation-dependent weighting and the Dry Niell troposphere model (Niell, 2000) to estimate site-specific troposphere parameters. The QIF quasi-ionosphere-free resolution strategy (Dach et al., 2007) was applied for ambiguity resolution. The high-rate kinematic coordinate results were based on L3 quasi-ionosphere-free linear combination of GPS frequencies. From the kinematic coordinates, three-dimensional, unfiltered, 1 Hz, displacement vector field animations were created. Individual 1 sec. frames were generated using the Generic Mapping Tools (Wessel & Smith, 1995), and the movies from these frames were generated with FFmpeg (ffmpeg.org) on the Ubuntu platform.

To assess the noise in the results, we processed the same time interval from the preceding day. The standard deviations of a normal distribution fit to the 1 Hz kinematic displacement were 3.6, 3.2 and 5.5 mm for the radial (42° azimuth), transverse and vertical components (Figure 1). The dynamic displacements from the seismic waves were an order of magnitude larger across the network (Figure 1, Video S1). Propagation of the wave field across the basin is shown along a NE–SW profile parallel to the surface-wave path from the epicentre. As the DD processing method is relative, GPS stations closer to the reference site NIZS – farthest from the epicenter – have smaller relative wave amplitudes.

3 | RESULTS AND DISCUSSION

The Tohoku earthquake's hypocentre was at 38°6.2′ N, 142°51.6′ E and 24 km depth, and its origin time was 05:46:24 UTC (Japan Meteorological Agency). The first clear arrival is shear waves causing NE horizontal displacement across the network starting at 6:08 UTC (Figure 1, Video S1). The largest displacement occurred at 6:08:33 with 17 mm amplitude. We interpret this signal as a combination of the S, sS, SKS and ScS body-wave phases, which should arrive only a few seconds apart. This interpretation is consistent with the transverse particle motion perpendicular to the direction of propagation. The NE–SW horizontal motion appears at essentially the same time across the basin, suggesting overall near-vertical incidence. Shear waves arriving around 6:11 UTC, also causing dominantly NE–SW

horizontal displacements, show deformation propagating within the basin at a large (7–8.5 km/s) apparent velocity (Figure 1c top right insert). GPS data indicate that the 6:11 UTC transverse motion reaches the NE part of the basin – closer to the epicentre – earlier, due to the probably larger incidence, and the mostly radial horizontal surface motions clearly advance to the SW. The largest relative displacement at 6:11:18 UTC in the NE direction is twice as large (34 mm) as the earlier arrival, whereas the largest SW displacement (20 mm) caused by the shear wave occurred at 6:12:06. Deformation signals between 6:15 and 6:17 are likely due to various S phases.

The horizontally polarized Love wave arrives at ~06:20:10. Its group velocity across the network is 4.1 ± 0.3 km/s as calculated from time/distance differences at several GPS site pairs within the basin, whereas the average path velocity, calculated from the origin time to the arrival at the GPS stations over the ~8800–9200 km minor arc distances is around 4.32 ± 0.02 km/s. ¼ wavelength of the observed Love wave is ~50 s, corresponding to a wavelength of approximately 850 ± 150 km. These displacements occur around half a minute later than IASP91 (Kennett & Engdahl, 1991) predicts. According to a global group velocity model (Larson & Ekström, 2001), a 175s Love wave has on average 1%–2% greater velocities across the major part of the ~9000 km minor arc over continental Eurasia than the global reference (Dziewonski & Anderson, 1981). This may reflect the fact that the moment rate increased significantly (Maercklin, Festa, Colombelli, & Zollo, 2012) more than half a minute after rupture initiation, making the later portion more visible. The horizontal motion caused by the Love wave reaches its NW maximum of 38 mm at 6:21:11 at VASA station, whereas the largest relative SE displacement – 48 mm – is observed at PUSP at 6:22:43. The propagation of the Love wave deformation is clearly observed – due to favourable directivity, soil structure etc. – having on average a ~70 mm peak-to-peak displacement even at more than 9000 km epicentral distance (Figure 2, Video S1).

As GPS positions are less accurate in the vertical direction, geodetic observation of Rayleigh surface waves at teleseismic distances was more challenging. However, given the earthquake's large magnitude, the ellipsoidal motion due to the Rayleigh wave is well recorded (Figure 3 and Video S1) even at this large, 78.8–82.3°,

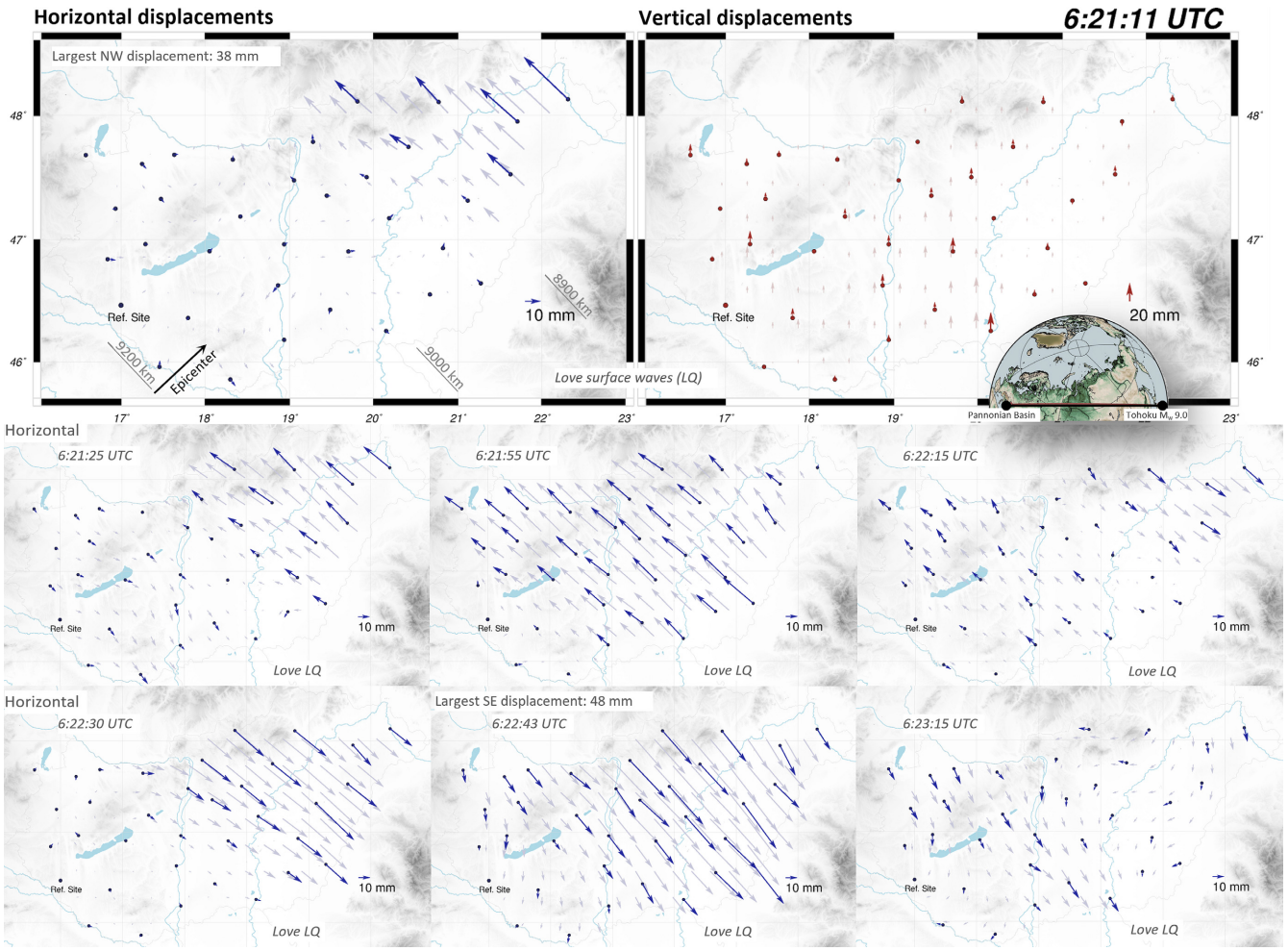

FIGURE 2 Passage of Love surface wave. Upper row: three-dimensional displacements when Love wave enters the basin. Direction and distance to the epicentre are indicated. Middle and lower rows from left to right: evolution of horizontal deformation (See Video S1 from 6:20 UTC). Black arrows are real unfiltered GPS data, light grey arrows are interpolated displacement field

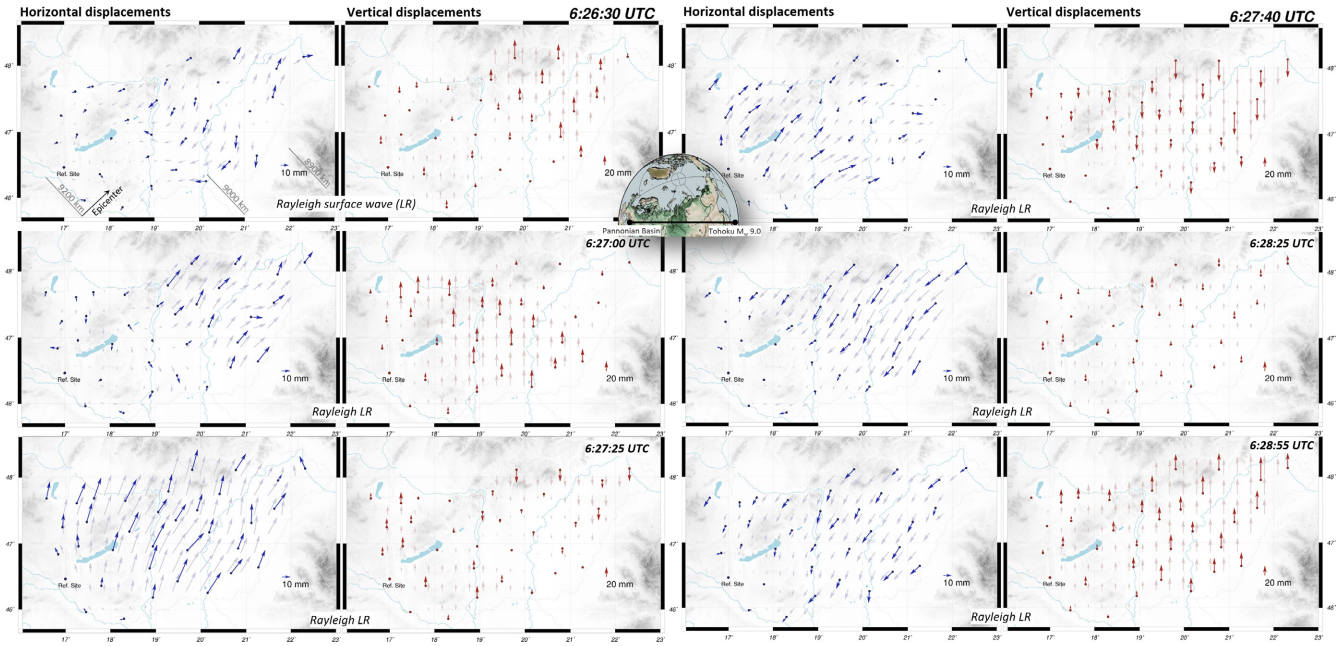

FIGURE 3 Three-dimensional GPS displacement vector field of the Rayleigh wave. Horizontal and vertical displacement field snapshots of a directly measured unfiltered 1 Hz vector field animation. The typical ellipsoidal-motion Rayleigh surface wave can be followed in 3D from the top left corner down in two columns. (See also Video S1 from 6:26 UTC)

epicentral distance. The Rayleigh wave first appears just before 6:25. Ellipsoidal motion starts with a small SW radial horizontal motion and insignificant downward motion. Less than a minute later significant uplift, reaching 40 mm, together with NE–SW radial lateral displacements appear; the largest peak-to-peak motion observed was 89 mm in the vertical direction and more than 60 mm in the horizontal direction. From the GPS data, we estimated 3.7 ± 0.3 km/s for the propagation velocity of the Rayleigh wave within the basin. The total path velocity is 3.79 ± 0.03 km/s based on the epicentral distances, the arrivals and the origin time. This arrival of the Rayleigh wave is also significantly later than predicted by IASP91, despite Rayleigh wave global group velocity models (Ma & Masters, 2014) indicating on average ~2%–3% greater velocity across the major part of the ~9000 km minor arc over continental Eurasia. As for the Love wave, this may reflect the moment release. The largest downward motion occurred at 6:27:40 with −45 mm, and the largest upward motion at 6:28:56 was 51 mm. The peak horizontal crustal deformation caused by the Rayleigh wave in the NE direction was 32 mm at 6:27:30 UTC, and in the SW direction it was 34 mm at 6:28:04 UTC. The average peak-to-peak ~NE–SW horizontal motion of the Rayleigh wave is ~50 mm, around 85% of the ~NW–SE Love horizontal displacements.

The GPS displacements have waveforms similar to, but not identical to, those recorded on nearby broadband seismometers. The differences presumably reflect the fact that most GPS sites in the network are on pillars atop multi-story buildings, giving larger displacements, as well as the effect of filtering on the seismic data and the effect of the DD GPS processing (Data S1).

Because the minor arc surface waves caused large transient strains, we looked to see whether their dynamic deformations triggered any seismic events in the Pannonian Basin. The Love wave resulted in 35 mm relative displacement over a distance of 125 km within 40 seconds, which corresponds to a 2.2×10^8 ppb/yr transient strain rate. This is a hundred million times the secular 3.5 ppb/yr tectonic contraction rate for the Pannonian basin (Grenerczy, Sella, Stein, & Kenyeres, 2005). Within the basin, an M = 4.5 earthquake – which on average occurs once in 10 years – happened at Oroszlány (Tóth, Mónus, Zsíros, Kiszely, & Czifra, 2012) on 29th January 2011, and the associated aftershocks dominate the seismicity statistics in March. After eliminating these aftershocks, increased seismicity was not observed, indicating that the transient strain did not trigger seismicity inside the basin.

We also detected the dynamic deformation caused by the Love wave (G2) that travelled around the Earth along the major arc, arriving from the opposite direction. This is the most distant earthquake wave displacement field geodetically observed to date. Based on the IASP91 model, we expect this around 117 min. 29 sec. after the origin, corresponding to 7:43:53 at GPS site NIZS. Being the furthest for G1 observations, now the G2 Love wave hits the GPS reference site first. Just before 7:44:00 this wave (Figure 4, Video S2) arrives with the expected NW–SE horizontal motion mapped with 1 sec temporal resolution across the network. The largest relative NW displacement of 18 mm is observed at NYL2 and the largest SE motion detected is 17 mm at VASA. G2 has less than 50% (47%–35%) of the displacement of the minor arc (G1) wave.

Our results show that GPS seismology is practical at much larger source–receiver distances than have been used to date. The complete

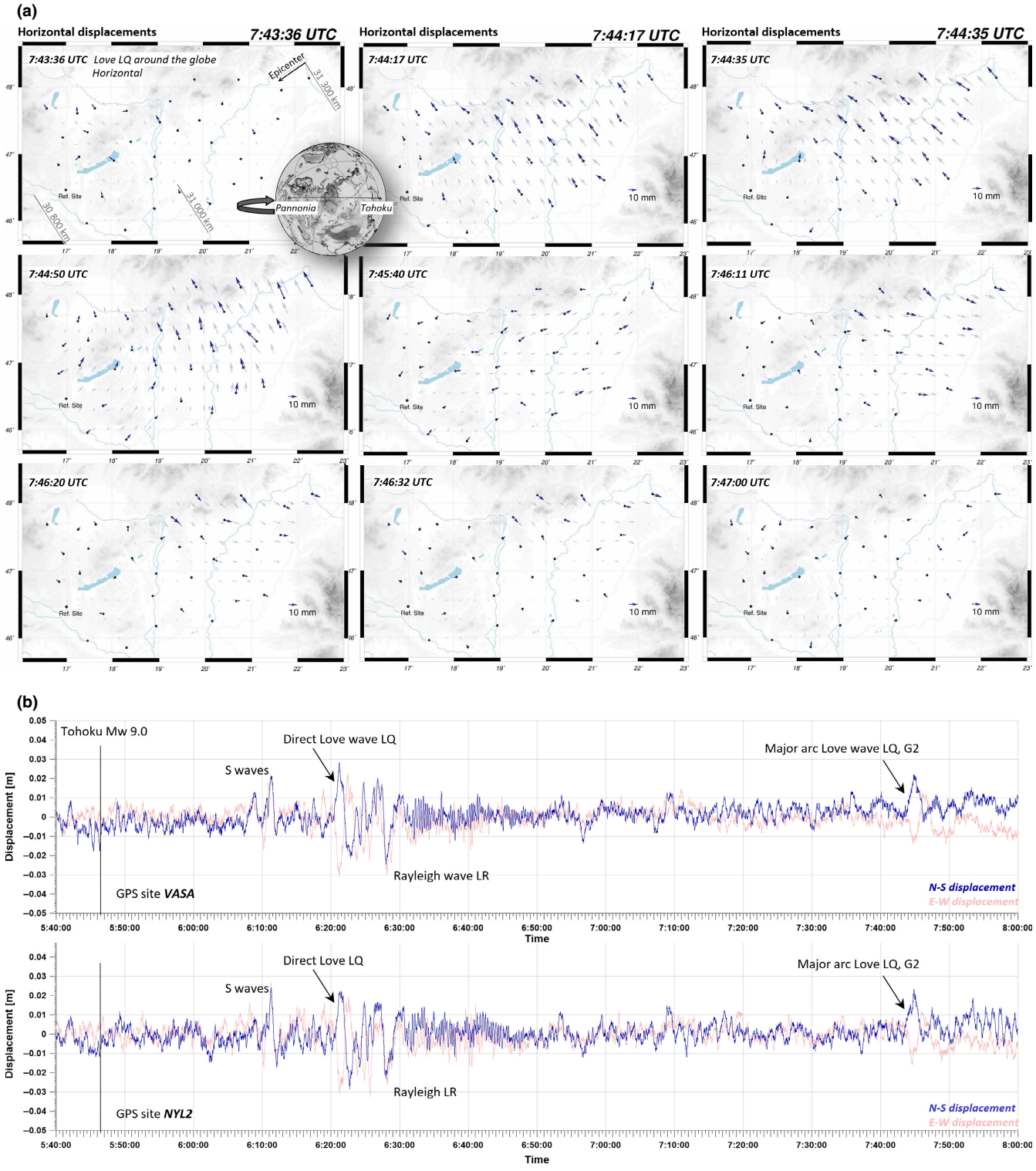

FIGURE 4 Evolution of horizontal dynamic deformation caused by the major arc (G2) Love wave from 31 000 km epicentral distance. Horizontal time series of two GPS stations. Black is N–S, light grey is E–W. (See Video S2 from 7:43 UTC)

three-dimensional 1 Hz GPS observation of the displacement vector fields of several body and surface waves at these large distances suggests that global space geodetic mapping of the dynamic response to great earthquakes is feasible. The seismic wavefield data from the rapidly growing number of real time kinematic GPS networks can be used for both teleseismic source studies and structural investigations. Although there are already a significant number of freely available high-rate GPS sites distributed globally (Houlié et al., 2011), the

continuously operating GPS networks in Europe and elsewhere are for real-time kinematic surveying and generally not freely accessible. Nonetheless, 3–4 hours of 1 Hz GNSS data could be made available for scientific purposes after large earthquakes without impacting their commercial value under a Supersite-type activity (Amelung et al., 2011). Such datasets together with stand-alone solutions (Colosimo, 2013) would open up the possibility of space geodetic mapping of the transient deformation field globally. Besides the near-field timely and more accurate magnitude estimates (Wright, Houlié, Hildyard, & Iwabuchi, 2012), valuable contributions to tsunami warning (Blewitt et al., 2009) and improved understanding of the rupture process (Avallone et al., 2011; Ozawa et al., 2011), far-field data could give new details of wave propagation and velocity structure that could be compared with data from other seismological methods, including global tomography (Romanowicz, 2003), and could contribute to high resolution regional and global petrophysical inversion (Lebedev, Boonen, & Trampert, 2009).

ACKNOWLEDGMENT

We thank Zoltán Gráczer and László Tóth from the Kövesligethy Radó Seismological Observatory of the Hungarian Academy of Science for valuable discussions. The authors are grateful for the constructive comments and suggestions of Jeff Freymueller at University of Alaska and an anonymous reviewer. The raw observational data are accessible from http://utolagos.gnssnet.hu/ The authors declare no conflicts of interest.

ORCID

Gyula Grenerczy http://orcid.org/0000-0002-1061-2209
Seth Stein http://orcid.org/0000-0003-0522-7418

REFERENCES

Altamimi, Z., Collilieux, X., Legrand, J., Garayt, B., & Boucher, C. (2007). ITRF2005: A new release of the International Terrestrial Reference Frame based on time series of station positions and Earth Orientation Parameters. *Journal of Geophysical Research*, *112*, B09401. https://doi.org/10.1029/2007JB004949

Amelung, F, Cocco, M., Dobson, C., Wright, T., Aoki, Y., Furuya, M. ... Meertens, C. (2011). Geohazard Supersites and Natural Laboratories Strategic Plan, Version 1.0, http://www.earthobservations.org/documents/

Avallone, A., Marzario, M., Cirella, A., Piatanesi, A., Rovelli, A., Di Alessandro, C. ... Mattone, M. (2011). Very high rate (10 Hz) GPS seismology for moderate-magnitude earthquakes: The case of the Mw 6.3 L'Aquila (central Italy) event. *Journal of Geophysical Research*, *116*, B02305. https://doi.org/10.1029/2010JB007834

Blewitt, G., Kreemer, C., Hammond, W.C., Plag, H.P., Stein, S. & Okal, S. (2009). GPS for real-time earthquake source determination and tsunami warning systems. *Journal of Geodesy*, *83*, 335–343. https://doi.org/10.1007/s00190-008-0262-5

Colosimo, G., (2013). *VADASE: A brand-new approach to real-time GNSS seismology*, 180 pp., ISSN:9783845438382, Saarbrücken, Germany: Lambert Academic Publishing AG & Co KG.

Dach, R., Hugentobler, U., Fridez, P., & Meindl, M. (2007). *Bernese GPS Software Version 5.0*. Bern, Switzerland. Astronomical Institute, University of Bern.

Dziewonski, A. M., & Anderson, D. L. (1981). Preliminary reference Earth model. *Physics of the earth and planetary interiors*, *25*, 297–356.

Elósegui, P., Davis, J. L., Oberlander, D., Baena, R., & Ekström, G. (2006). Accuracy of high-rate GPS for seismology. *Geophysical Research Letters*, *33*, L11308. https://doi.org/10.1029/2006GL026065

Emore, G., Haase, J., Choi, K., Larson, K. M., & Yamagiwa, A. (2007). Recovering absolute seismic displacements through combined use of 1-Hz GPS and strong motion accelerometers. *Bull Seism Soc Am*, *97*, 357–378. https://doi.org/10.1785/0120060153

Grapenthin, R., & Freymueller, J. T. (2011). The dynamics of a seismic wave field: Animation and analysis of kinematic GPS data recorded during the 2011 Tohoku-oki earthquake, Japan. *Geophysical Research Letters*, *38*, L18308. https://doi.org/10.1029/2011GL048405

Grenerczy, G., Sella, G., Stein, S., & Kenyeres, A. (2005). Tectonic implications of the GPS velocity field in the northern Adriatic region. *Geophysical Research Letters*, *32*, L16311. https://doi.org/10.1029/2005GL022947

Hardebeck, J. L., Boatwright, J., Dreger, D., Goel, R., Graizer, V., Hudnut, K., & Tinsley, J. C. (2004). Preliminary report on the 22 December 2003, m 6.5 San Simeon, California earthquake. *Seismological Research Letters*, *75*, 155–172.

Hirahara, K., Nakano, T., Hoso, Y., Matsuo, S., & Obana, K. (1994). *An experiment for GPS strain seismometer*, In: Japanese Symposium on GPS, 15-16 December, Tokyo, Japan, National Academy. pp:67–75.

Houlié, N., Occhipinti, G., Blanchard, T., Shapiro, N., Lognonné, P., & Murakami, M. (2011). New approach to detect seismic surface waves in 1Hz-sampled GPS time series. *Scientific Reports*, *11*, 44.

Kennett, B. L. N, & Engdahl, E. R. (1991). Traveltimes for global earthquake location and phase identification, *Geophysical Journal International*, *105*, pp 429–465.

Kouba, J. (2005). A possible detection of the 26 December 2004 Great Sumatra-Andaman Islands Earthquake with solution products of the International GNSS Service. *Studia Geophysica et Geodaetica*, *49*, 463–483.

Larson, K. M., Bodin, P., & Gomberg, J. (2003). Using 1-Hz GPS data to measure deformations caused by the Denali fault earthquake. *Science*, *300*, 1421–1424. https://doi.org/10.1126/science.1084531

Larson, E. W. F., & Ekström, G. (2001). Global Models of Surface Wave Group Velocity, Pure Appl. *Geophys*. *158*, 1377–1400.

Lebedev, S., Boonen, J., & Trampert, J., (2009). Seismic structure of Precambrian lithosphere: New constraints from broadband surface-wave dispersion, *Lithos*, *109*, 96–111.

Lyard, F., Lefevre, F., Letellier, T., & Francis, O. (2006). Modelling the global ocean tides: Modern insights from FES2004. *Ocean Dynamics*, *56*, 394–415. https://doi.org/10.1007/s10236-006-0086

Ma, Z., & Masters, G. (2014). A New Global Rayleigh-and Love-Wave Group Velocity Dataset for Constraining Lithosphere Properties. *Bulletin of the Seismological Society of America*, *104*, 2007–2026.

Maercklin, N., Festa, G., Colombelli, S., & Zollo, A., (2012). Twin ruptures grew to build up the giant 2011 Tohoku, Japan, earthquake. *Scientific Reports*. *2*:709.

Miyazaki, S., Larson, K., Choi, K., Hikima, K., Koketsu, K., Bodin, P. ... Yamagiwa, A. (2004). Modeling the rupture process of the 2003 Tokachi-Oki earthquake using 1-Hz GPS data. *Geophysical Research Letters*, *31*, L21603. https://doi.org/10.1029/2004GL021457

Nettles, M., Ekström, G., & Koss, H. C. (2011). Centroid-moment-tensor analysis of the 2011 off the Pacific coast of Tohoku Earthquake and its larger foreshocks and aftershocks. *Earth, Planets and Space*, *63*, 519–523.

Niell, A. E. (2000). Improved atmospheric mapping functions for VLBI and GPS. *Earth, Planets and Space*, *52*, 699–702.

Ozawa, S., Nishimura, T., Suito, H., Kobayashi, T., Tobita, M. ... Imakiire, T. (2011). Coseismic and postseismic slip of the 2011 magnitude-9 Tohoku-Oki earthquake. *Nature*, *475*, 373–376.

Romanowicz, B. (2003). Global mantle tomography: Progress status in the past 10 years. *Annual Review of Earth and Planetary Sciences*, *31*, 303–328.

Tóth, L., Mónus, P., Zsíros, T., Kiszely, M., & Czifra, T. (2012). *Magyarországi földrengések évkönyve-Hungarian Earthquake Bulletin–2011*, GeoRisk, Budapest, 158 oldal, HU ISSN. 1589–8326.

Vigny, C., Simons, W. J., Abu, S., Bamphenyu, R., Satirapod, C., Choosakul, N., & Ambrosius, B. A. C. (2005). Insight into the 2004 Sumatra-Andaman earthquake from GPS measurements in Southeast Asia. *Nature*, *436*, 201–206.

Wessel, P., & Smith, W. H. F. (1995). New version of the Generic Mapping Tools released. *Eos Transactions American Geophysical Union*, *76*, 329.

Wright, T. J., Houlié, N., Hildyard, M., & Iwabuchi, T. (2012). Real-time, reliable magnitudes for large earthquakes from 1 Hz GPS precise point positioning: The 2011 Tohoku-Oki (Japan) earthquake. *Geophysical Research Letters*, *39*, L12302. https://doi.org/10.1029/2012GL051894

SUPPORTING INFORMATION

Additional Supporting Information may be found online in the supporting information tab for this article.

Data S1 Comparison of space geodetic and seismological displacement signals after the 2011 March 11 Mw 9.0 Tohoku earthquake at GPS site VASA and TARPA broadband seismological station.

Video S1 a Three-dimensional, space geodetic, directly measured, unfiltered, 1 Hz, displacement vector field animation of dynamic deformation caused by G1 minor arc seismic waves of the 2011 Tohoku earthquake at 9000 km epicentral distance. (30fps)

Video S1 b The same as Video S1 a but longer, slower 10 frame per second video for better visual analysis.

Video S2 Two-dimensional, space geodetic, directly measured, unfiltered, 1 Hz, displacement vector field animation of dynamic deformation caused by G2 major arc Love wave of the 2011 Tohoku earthquake at 31 000 km epicentral distance.

How to cite this article: Grenerczy G, Jámbor T, Stein S, Farkas P, Ferenc M. Towards global space geodetic mapping of the dynamic deformation field after great earthquakes. *Terra Nova*. 2017;00:1–7. https://doi.org/10.1111/ter.12301